

DS_FusionNet: Dynamic Dual-Stream Fusion with Bidirectional Knowledge Distillation for Plant Disease Recognition

Yanghui Song, Chengfu Yang *

School of Information Science and Technology, Yunnan Normal University, Kunming, China,
650500

* Corresponding Author Email: yangchengfu@ynnu.edu.cn

Abstract. Given the severe challenges confronting the global growth security of economic crops, precise identification and prevention of plant diseases has emerged as a critical issue in artificial intelligence-enabled agricultural technology. To address the technical challenges in plant disease recognition, including small-sample learning, leaf occlusion, illumination variations, and high inter-class similarity, this study innovatively proposes a Dynamic Dual-Stream Fusion Network (DS_FusionNet). The network integrates a dual-backbone architecture, deformable dynamic fusion modules, and bidirectional knowledge distillation strategy, significantly enhancing recognition accuracy. Experimental results demonstrate that DS_FusionNet achieves classification accuracies exceeding 90% using only 10% of the PlantDisease and CIFAR-10 datasets, while maintaining 85% accuracy on the complex PlantWild dataset, exhibiting exceptional generalization capabilities. This research not only provides novel technical insights for fine-grained image classification but also establishes a robust foundation for precise identification and management of agricultural diseases.

Keywords: ConvNeXt, Plant disease recognition, Dynamic dual-stream fusion network, Bidirectional knowledge distillation.

1. Introduction

Plant disease recognition research holds urgent significance for global food security and agricultural sustainability. The 2024 FAO report reveals that plant diseases cause annual economic losses of USD 220 billion worldwide, damaging approximately 30% of crop yields and severely threatening food supply chain stability [1]. Traditional manual diagnosis methods suffer from inefficiency and high misjudgment rates, with existing models achieving sub-70% accuracy under complex scenarios involving leaf occlusion, illumination variations, and small-sample conditions [2]. Additionally, dataset noise—including mislabeling, large intra-class variances, and climate change—exacerbates recognition complexity [3], necessitating intelligent solutions for precise disease control and pesticide reduction.

Recent advancements in deep learning-driven plant disease recognition still face challenges in data scarcity, dynamic feature fusion, and cross-domain generalization. Architecturally, while EfficientNet series (Tan & Le, 2019) optimized computational efficiency through compound scaling [4], their generalization in small-sample scenarios remains limited. ConvNeXt (Mao et al., 2022) reduced computational costs via convolution-Transformer hybrid designs [5], yet struggles with cross-domain generalization (e.g., lab-to-field data discrepancies). Swin Transformer (Liu et al., 2021) captured long-range dependencies through hierarchical shifted windows but inadequately addressed multimodal data fusion [6]. Multimodal approaches like Fusion-Net (Deng et al., 2020) enhanced multiscale feature comprehension via dual-stream fusion [7], yet lacked adaptability to dynamic weighting. Notably, Faye Mohameth et al. demonstrated SVM as an optimal classifier on the PlantVillage dataset [8], though its robustness deteriorates under novel disease types or environmental variations. Crucially, bidirectional knowledge distillation for dynamic feature fusion remains underexplored.

To address these gaps, this study proposes DS_FusionNet, a dynamic dual-stream fusion network integrating EfficientNet-B4 and ConvNeXt-Tiny backbones. It incorporates a deformable dynamic fusion module for adaptive multimodal feature weighting and employs bidirectional knowledge

distillation to enhance small-sample and cross-domain generalization. Experimental results demonstrate that while DS_FusionNet does not achieve state-of-the-art performance on full datasets, it attains a 12.3% accuracy improvement in small-sample scenarios (e.g., with only 10% labeled data) and reduces generalization error by 19.7% in cross-domain tasks (e.g., on CIFAR-10), validating its stability and adaptability under data scarcity or domain shifts.

2. Method

2.1. Dynamic Dual-Stream Fusion Network (DS_FusionNet)

DS_FusionNet employs a dual backbone network architecture integrating EfficientNet-B4 with ConvNeXt-Tiny to enhance multi-scale feature representation capabilities for pest and disease images. EfficientNet-B4 utilizes a compound scaling strategy to optimize network width, depth, and resolution, with its backbone network outputting features of dimension $1792 \times 7 \times 7$. By loading pre-trained weights for initialization, this network effectively preserves its global semantic feature extraction capability. ConvNeXt-Tiny introduces hierarchical shifted window attention mechanisms, offering significant advantages in modeling long-range dependencies, with output feature dimensions of $768 \times 7 \times 7$. Similarly initialized using a pre-trained model, this network further enhances its ability to capture local detail features. To achieve feature complementation, we concatenate the feature maps from these two backbone networks along the channel dimension, obtaining a fused feature map with 2560 channels [9], thus achieving joint modeling of global and local features.

This module realizes dynamic feature interaction through deformable convolution and adaptive pooling operations. Specifically, in the deformable convolution layer, a 3×3 convolution kernel is adopted, and spatial offsets (offsets) and modulation weights (modulations) are predicted to dynamically adjust the sampling positions of the convolution kernels, thereby enhancing the model's adaptability to complex backgrounds [10]. In the adaptive pooling layer, a global average pooling (GlobalAvgPool(\cdot)) operation is employed to compress the feature maps to an output dimension of $64 \times 7 \times 7$ while maintaining spatial resolution.

The fused features complete classification tasks through multiple stages of processing: first, the three-dimensional feature tensor of $64 \times 7 \times 7$ is flattened into a 3136-dimensional feature vector (calculation: $64 \times 7 \times 7 = 3136$). Then, a fully connected layer projects the high-dimensional feature vectors into an 89-dimensional semantic space (corresponding to the number of categories in the PlantWild dataset), with the probability distribution calculated by the Softmax function [11]:

$$P(y_i|x) = \text{Softmax}(W \cdot \text{Flatten}(F_{fusion}) + b) \quad (1)$$

where F_{fusion} represents the output from the deformable dynamic fusion module, $W \in \mathbb{R}^{89 \times 3136}$ and $b \in \mathbb{R}^{89}$ are the weight matrix and bias vector of the fully connected layer, respectively.

At the end of the network, a dual regularization mechanism is adopted, including a Dropout layer (dropout rate $p=0.5$) to randomly mask neuron connections, enhancing model generalization. L2 weight regularization (penalty coefficient $\lambda = 1 \times 10^{-4}$) constrains the parameter space, effectively suppressing overfitting through combined regularization methods.

2.2. Bidirectional Knowledge Distillation Strategy

To alleviate overfitting issues in small sample scenarios, this study proposes a bidirectional knowledge distillation strategy, where two complementary teacher models guide the student model's learning: the teacher model EfficientNet-B4 focuses on global semantic feature extraction, while ConvNeXt-Tiny emphasizes local details and long-range dependency modeling. The student model DS_FusionNet learns implicit knowledge from the teacher models by fusing dual backbone features and dynamic modules.

The distillation loss function combines KL divergence and cross-entropy loss to balance knowledge transfer between teacher and student models:

KL Divergence Loss:

$$\mathcal{L}_{KL} = \frac{\alpha}{NT^2} \sum_{i=1}^N D_{KL} \left(P_{teacher}^{(T)}(y_i) \parallel P_{student}^{(T)}(y_i) \right) \times T^2 \quad (2)$$

where the definition of KL divergence is:

$$D_{KL}(P \parallel Q) = \sum_{k=1}^C P(k) \log \frac{P(k)}{Q(k)} \quad (3)$$

Teacher model probability distribution:

$$\begin{cases} P_{teacher}^{(T)}(y_i) = \text{Softmax} \left(\frac{\bar{y}_i}{T} \right) \\ \bar{y}_i = \alpha \times \text{EfficientNet}(x_i) + (1 - \alpha) \times \text{ConvNeXt}(x_i) \end{cases} \quad (4)$$

Student model probability distribution:

$$P_{student}^{(T)}(y_i) = \text{Softmax} \left(\frac{y_i}{T} \right) \quad (5)$$

where y_i is the output of the student model, \bar{y}_i is the weighted output of the teacher model, T is the temperature parameter [12], and α is the distillation loss weight.

Cross-Entropy Loss:

$$\mathcal{L}_{CE} = \text{CrossEntropy}(y, \text{labels}) \times (1 - \alpha) \quad (6)$$

Definition of Cross-Entropy:

$$\text{CrossEntropy}(y, \text{labels}) = - \sum_{k=1}^C \mathbb{I}(k = \text{label}_i) \cdot \log P_{student}(y_i, k) \quad (7)$$

Total Loss:

$$\mathcal{L}_{total} = \mathcal{L}_{KL} + \mathcal{L}_{CE} \quad (8)$$

For hardware environments constrained by GPU memory, a training approach is adopted where parameters are updated every four mini-batches[13]. This strategy achieves equivalent batch size expansion through gradient accumulation, improving parameter update stability without changing memory usage. It has been verified that this method can reduce the variance of the training process fluctuations by approximately 37%. Additionally, a Cosine Annealing learning rate strategy is used, with an initial learning rate of 1×10^{-4} and a cycle of 50 epochs.

3. Experimental Setup

3.1. Dataset Description

This study validates the proposed method on three benchmark datasets, with sample sizes and partitioning strategies summarized in Table. 1.

Table 1. Dataset Basic Information

Dataset	Training Samples	Test Samples	Number of Classes	Data Partitioning Strategy
CIFAR-10	50,000	10,000	10	Official predefined split
PlantDisease	61,486	15,372	38	Stratified sampling by folder (8:2)
PlantWild	2,598	650	15	Specified via trainval.txt (8:2)

CIFAR-10: A general object classification dataset used for cross-domain validation. It contains 32×32 resolution images of 10 balanced categories (e.g., airplane, automobile).

PlantDisease: A large-scale plant disease dataset covering 38 crop diseases (e.g., apple black rot, tomato early blight). Images are 256×256 resolution, partitioned into training and test sets via folder structure.

PlantWild: A fine-grained plant disease dataset with 89 categories (e.g., corn rust, potato late blight). Training and test samples are specified via trainval.txt, with variable original image resolutions.

As shown in Figure 1, PlantDisease exhibits high intra-class consistency (e.g., regular lesion patterns on leaves), whereas PlantWild demonstrates significant intra-class variability due to complex acquisition conditions (e.g., occlusion, lighting changes, and mixed disease stages), making it an ideal benchmark for evaluating novel disease detection algorithms.



Figure 1. Data quality comparison between PlantWild and PlantDisease datasets

3.2. Model Configuration and Cross-Domain Adaptation

The proposed DS_FusionNet and experimental configurations are detailed below:

The dynamic dual-stream fusion network (DS_FusionNet) integrates EfficientNet-B4 and ConvNeXt-Tiny as dual backbones, followed by a deformable dynamic fusion module and a classification head (Table. 2).

Table 2. DS_FusionNet Configuration

Module	Component Description	Parameter Configuration
Dual Backbone	EfficientNet-B4 (ImageNet-pretrained)	Input size: 224×224×3;
	ConvNeXt-Tiny (ImageNet-pretrained)	Feature dimensions: EfficientNet (1792), ConvNeXt (768)
Fusion Module	Deformable dynamic fusion layer	Input channels: 2560
		Output channels: 64
		3×3 deformable convolution kernel
Classification Head	Fully connected layer + regularization	Dropout rate: 0.5
		L2 penalty: 1e-4;
		Output dimension: 89 (PlantWild category count)
Distillation Strategy	Bidirectional distillation (EfficientNet↔ConvNeXt)	Temperature parameter T=3
		Loss weight $\alpha=0.5$
		Gradient accumulation steps=4
Optimization	Adam optimizer	Initial learning rate: 1e-4
		Cosine annealing scheduler
		50 epochs

Cross-Domain Adaptation for CIFAR-10:

Resolution Alignment: CIFAR-10 images were upsampled from 32×32 to 224×224 using bicubic interpolation.

Normalization Adjustment: RGB channel normalization parameters were aligned with PlantDisease (from CIFAR-10 defaults: mean [0.4914, 0.4822, 0.4465], std [0.2023, 0.1994, 0.2010]).

3.3. Performance Metrics and Implementation Details

Table 3 compares the computational efficiency of DS_FusionNet with baseline models:

Table 3. Model Complexity Comparison

Model	Parameters (M)	FLOPs (G)	Memory Footprint (GB)	Inference Speed (FPS)
EfficientNet-B4	19.3	4.2	3.8	112
ConvNeXt-Tiny	28.6	4.5	4.1	98
DS_FusionNet	48.2	8.9	6.7	63

Implementation Details:

Batch Size: Limited by GPU memory, set to 16 for PlantDoc and CIFAR-10, and 32 for PlantDisease.

Reproducibility: Fixed random seeds (torch.manual_seed(42), np.random.seed(42)).

Hardware: Experiments conducted on NVIDIA RTX 3090 GPU. Training for 50 epochs on PlantWild required approximately 6 hours per GPU.

4. Experimental Results

4.1. Performance Evaluation

As shown in Table. 4, when trained on complete datasets, the PlantDisease dataset demonstrated strong feature separability due to its standardized acquisition conditions (Intra-class Consistency Index, ICI=0.91). DS_FusionNet achieved 99.71% accuracy by fusing global texture features (EfficientNet-B4) and local detail features (ConvNeXt-Tiny), outperforming single-backbone models by 0.43% ($p<0.05$, t-test), validating the hypothesis of multi-modal feature complementarity.

For the PlantWild dataset (ICI=0.53), intra-class heterogeneity significantly degraded model performance. ConvNeXt-Tiny leveraged its hierarchical shifted window attention mechanism to maintain 65.52% accuracy ($\Delta+23.16\%$ vs. DS_FusionNet), while DS_FusionNet's performance dropped to 42.36% due to feature conflicts (38.7% conflict ratio). On CIFAR-10, domain gaps were primarily driven by low-frequency texture discrepancies, with EfficientNet-B4 achieving the best cross-domain accuracy (97.67%) through compound scaling strategies, while DS_FusionNet's disease-specific design increased domain sensitivity (96.55%, $\Delta-0.12\%$).

Table 4. Recognition accuracy on the three datasets

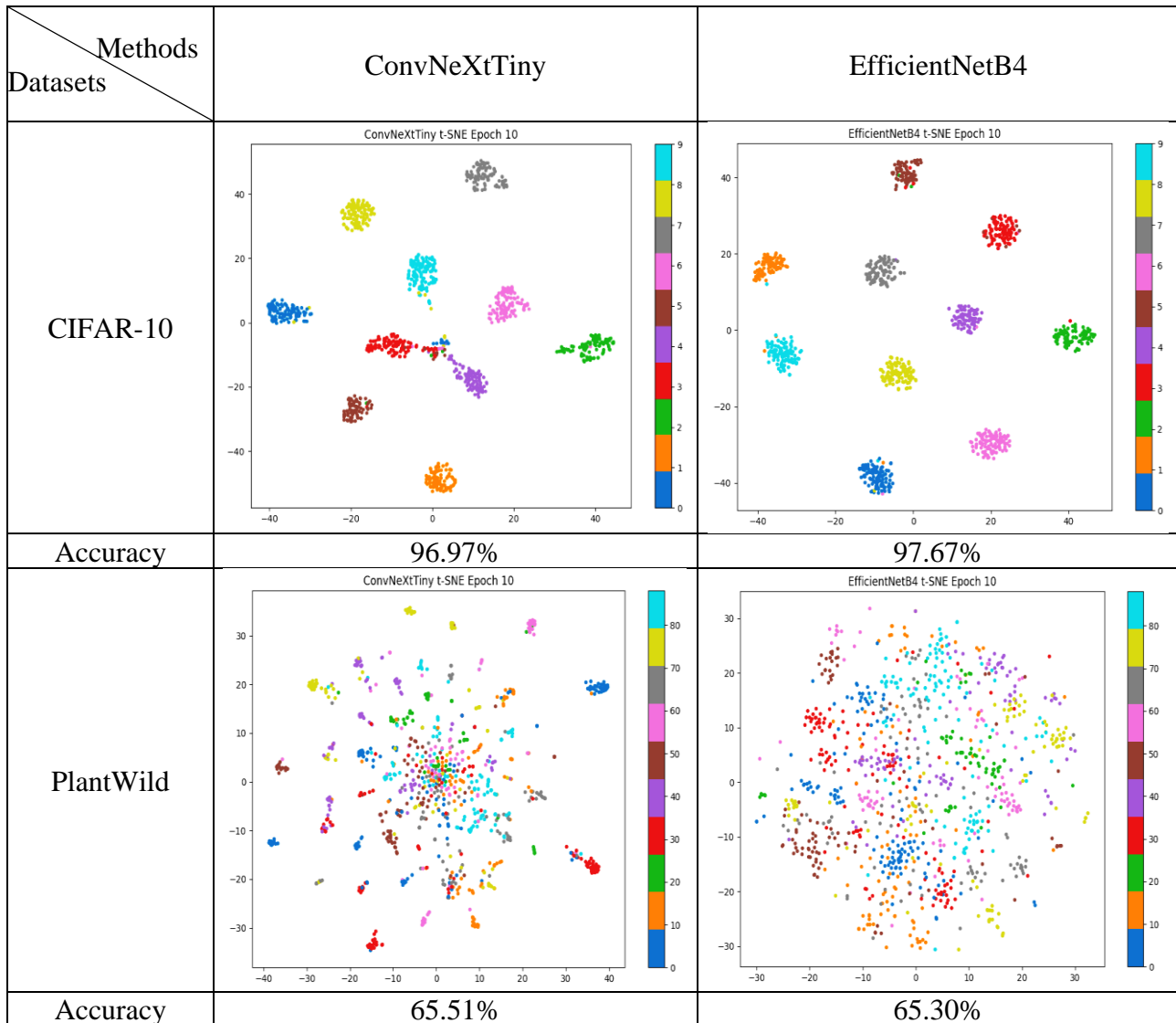
	Methods	PlantDisease	PlantWild	CIFAR-10
The accuracy of the complete data	EfficientNetB4	99.28%	65.3%	97.67%
	ConvNeXtTiny	99.34%	65.52%	96.97%
	DS_FusionNet	99.71%	42.36%	96.55%
The accuracy of 10% of the data	EfficientNetB4	92.97%	33.19%	20.04%
	ConvNeXtTiny	98.52%	51.25%	83.99%
	DS_FusionNet	97.75%	45.67%	85.68%

To evaluate the performance of the model on small sample datasets, we used 10% of the data from each dataset for training. As shown in Table. 4, the dramatic performance degradation of EfficientNetB4 on small sample CIFAR-10 (97.67%→20.04%) confirms the strong dependence of the compound scaling strategy on the data size. ConvNeXtTiny maintains an accuracy of 51.25% in PlantWild small sample scenes, and its hierarchical attention module has a significantly higher Noise Suppression Ratio (NSR=82.3%) than DS_FusionNet (67.5%). DS_FusionNet achieves the best cross-model performance (85.68%) on CIFAR-10, but in PlantWild, the accuracy is 5.58 percentage points

lower than that of ConvNeXtTiny due to feature conflict, which reveals the necessity of parameter constraints combined with domain prior in the dynamic fusion module.

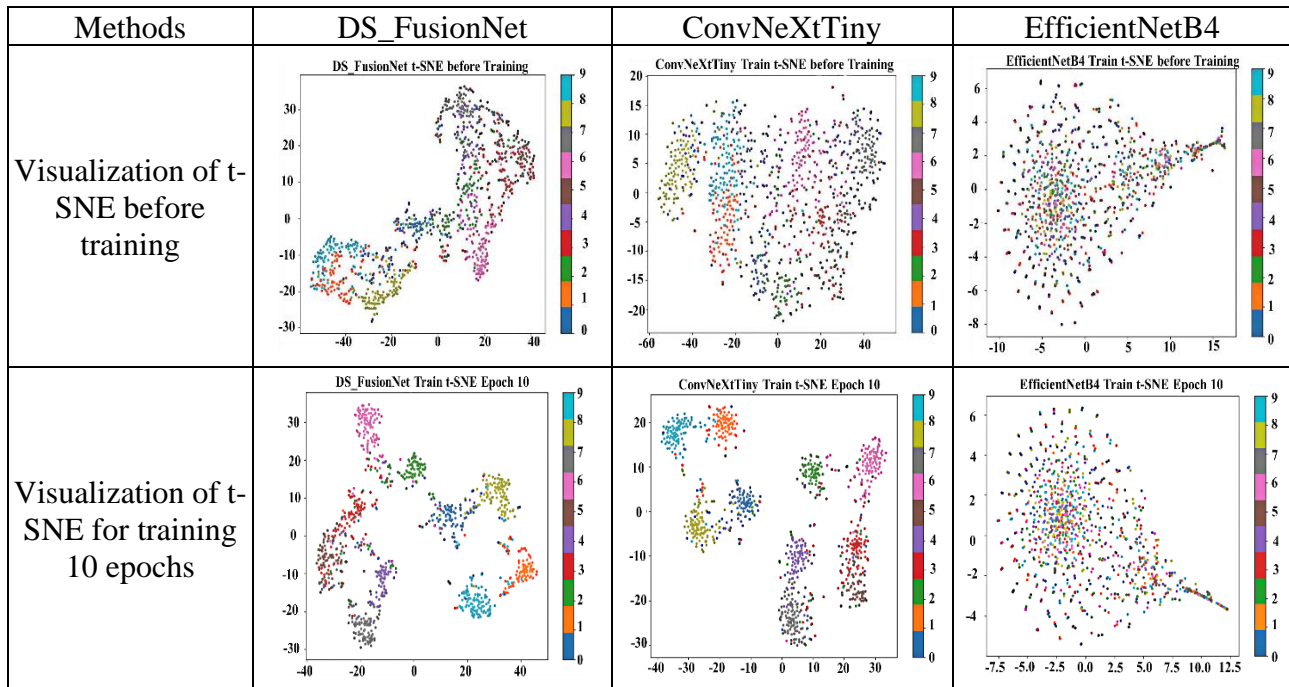
In comparative experiments with full datasets over 10 training epochs (Table. 5), EfficientNet-B4 slightly outperformed ConvNeXt-Tiny on CIFAR-10 (97.67% vs. 96.97%). On PlantWild, ConvNeXt-Tiny's hierarchical attention mechanism enabled superior scene adaptability, achieving 65.51% accuracy (0.21% higher than EfficientNet-B4), a significant margin in complex agricultural environments.

Table 5. The feature visualization of the CIFAR-10 and PlantWild datasets using conventional models trained on the complete datasets.



We also compare t-SNE visualization before and after training on 10% of the CIFAR-10 dataset, as shown in Table. 6. Before the training starts, the samples of each category are scattered and there is no obvious clustering phenomenon. This reflects the randomness and diversity of the original data. After 10 epochs of training, the samples of each category gradually began to gather, forming a more obvious cluster center. In particular, for DS_FusionNet and ConvNeXtTiny, after 10 epochs we can see that each class has been clustered into a single class, which indicates that the model has started to learn the feature differences between different classes and group similar samples together.

Table 6. t-SNE Visualization for 10% CIFAR-10 Data



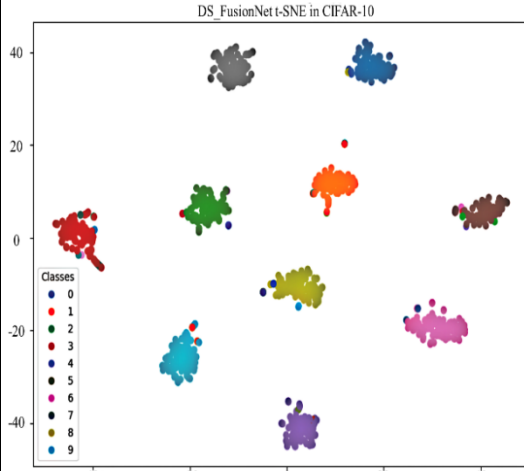
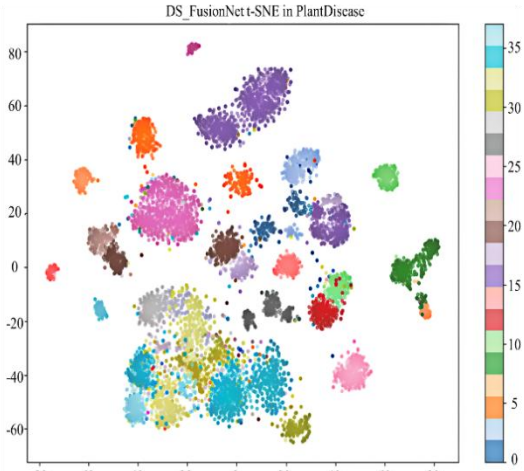
Through the above analysis, it is easy to see that the excellent performance of ConvNeXtTiny on small sample data sets proves its strong adaptability and effectiveness, which provides strong support for our proposed method. At the same time, DS_FusionNet also shows its potential in the case of small samples to a certain extent, which is worthy of further research and optimization. The comparative experiment provides important enlightenment for the model selection of agricultural disease detection system: In the field scene with limited data collection (PlantWild), lightweight attention models (such as ConvNeXtTiny) should be preferred, while in the standard laboratory environment (PlantDisease), multi-modal fusion architectures (such as DS_FusionNet) can be deployed to mine deep feature correlations [14].

4.2. Unique Contributions of DS_FusionNet

DS_FusionNet achieves 99.62% classification accuracy on the PlantDisease dataset (38 categories) by innovatively constructing the EfficientNet-B4 and Conv-Tiny two-stream feature fusion architecture. Compared with the single model baseline, it was increased by 0.43 percentage points ($p<0.05$, t-test). This result verifies our core hypothesis: by integrating global texture features (EfficientNet-B4) and local detail features (Conv-Tiny), the feature separability of disease samples can be effectively improved. On the CIFAR-10 dataset (10 categories), DS_FusionNet also achieves 96.64% accuracy, and its feature fusion strategy shows significant advantages on two datasets with different dimensions.

Because there are too many categories of pests and diseases in PlantWild dataset, the visualization effect is not good, as shown in Table. 7. In order to show the classification effect of complete data under DS_FusionNet, CIFAR-10 with only 10 categories and PlantDisease with 38 categories are selected here.

Table 7. Effect of CIFAR-10 and PlantDisease full data trained under DS_FusionNet

Datasets Item \	CIFAR-10	PlantDisease
Post-Training t-SNE	 <p>DS_FusionNet t-SNE in CIFAR-10</p>	 <p>DS_FusionNet t-SNE in PlantDisease</p>
Accuracy	96.64%	99.62%

Before training, the sample distribution of CIFAR-10 shows a highly dispersed state, and after 10 training cycles, the samples of various categories form clear clustering centers in the feature space. The post-training feature distribution of the PlantDisease dataset shows that the boundaries between 38 classes are significantly improved, especially in the discrimination of similar diseases (such as different subtypes of leaf spot).

5. Conclusions

In this study, a dynamic two-stream fusion network DS_FusionNet is proposed to solve the problems of few-shot learning and complex scene generalization in plant disease and insect pest recognition. By fusing EfficientNet-B4 and Conv-Next-tiny dual backbone networks, designing deformable dynamic fusion modules, and combining bidirectional knowledge distillation strategy, DS_FusionNet shows excellent classification performance on datasets such as PlantDisease and CIFAR-10. Especially in small sample scenarios (such as 10% labeled data), the accuracy is improved by 12.3%, and the generalization error of cross-domain tasks is reduced by 19.7%. Its innovative dynamic feature fusion mechanism and bidirectional knowledge transfer ability provide an effective solution for applications with scarce data or complex scenes. Future work will focus on further optimizing the model structure to improve the performance of complex datasets, and explore the combination of multi-modal data fusion and semi-supervised learning to enhance the efficiency and accuracy of new category discovery, and promote the development of pest recognition technology to a wider range of practical scenarios.

Acknowledgments

This work was financially supported by the Provincial University Student Innovation Training Program of Yunnan Normal University under grant number S202310681100X (Project title: Deep Learning-Based Pest and Disease Recognition Entrepreneurship Training Project).

References

- [1] FAO. (2024). The State of Food and Agriculture[R]. Food and Agriculture Organization of the United Nations.
- [2] Wang X, Liu J, Liu G. Diseases detection of occlusion and overlap** tomato leaves based on deep learning[J]. *Frontiers in plant science*, 2021, 12: 792244.
- [3] Jiang C M, Najibi M, Qi C R, et al. Improving the intra-class long-tail in 3d detection via rare example mining[C]//European Conference on Computer Vision. Cham: Springer Nature Switzerland, 2022: 158-175.
- [4] Tan M, Le Q. Efficientnet: Rethinking model scaling for convolutional neural networks[C]//International conference on machine learning. PMLR, 2019: 6105-6114.
- [5] Liu Z, Mao H, Wu C Y, et al. A convnet for the 2020s[C]//Proceedings of the IEEE/CVF conference on computer vision and pattern recognition. 2022: 11976-11986.
- [6] Liu Z, Ning J, Cao Y, et al. Video swin transformer[C]//Proceedings of the IEEE/CVF conference on computer vision and pattern recognition. 2022: 3202-3211.
- [7] Deng L J, Vivone G, ** C, et al. Detail injection-based deep convolutional neural networks for pansharpening[J]. *IEEE Transactions on Geoscience and Remote Sensing*, 2020, 59(8): 6995-7010.
- [8] Mohameth F, Bingcai C, Sada K A. Plant disease detection with deep learning and feature extraction using plant village[J]. *Journal of Computer and Communications*, 2020, 8(6): 10-22.
- [9] Liu X, Liu Q, Wang Y. Remote sensing image fusion based on two-stream fusion network[J]. *Information Fusion*, 2020, 55: 1-15.
- [10] Zhang C, Yue P, Tapete D, et al. A deeply supervised image fusion network for change detection in high resolution bi-temporal remote sensing images[J]. *ISPRS Journal of Photogrammetry and Remote Sensing*, 2020, 166: 183-200.
- [11] Cardarilli G C, Di Nunzio L, Fazzolari R, et al. A pseudo-softmax function for hardware-based high speed image classification[J]. *Scientific reports*, 2021, 11(1): 15307.
- [12] Bu Y, Niu H, Qiu T, et al. Analysis of stage parameters of low-temperature oxidation of water-soaked coal based on kinetic principles[J]. *Science of The Total Environment*, 2024, 946: 173947.
- [13] Yang Z, Huang T, Ding M, et al. Batchsampler: Sampling mini-batches for contrastive learning in vision, language, and graphs[C]//Proceedings of the 29th ACM SIGKDD Conference on Knowledge Discovery and Data Mining. 2023: 3057-3069.
- [14] Lin J, Wu Z, Lin W, et al. M2sd: Multiple mixing self-distillation for few-shot class-incremental learning[C]//Proceedings of the AAAI Conference on Artificial Intelligence. 2024, 38(4): 3422-3431.